

Atom interferometry and gravitational wave detection

Quantum Sensors for Fundamental Physics

QSFP School 2021

Jason Hogan
Stanford University
September 2021

Outline

Lecture 1

- General introduction/motivation
- Non-relativistic atom interferometer phase theory
- Example applications
- **Tutorial:** Accelerometer phase response

Lecture 2

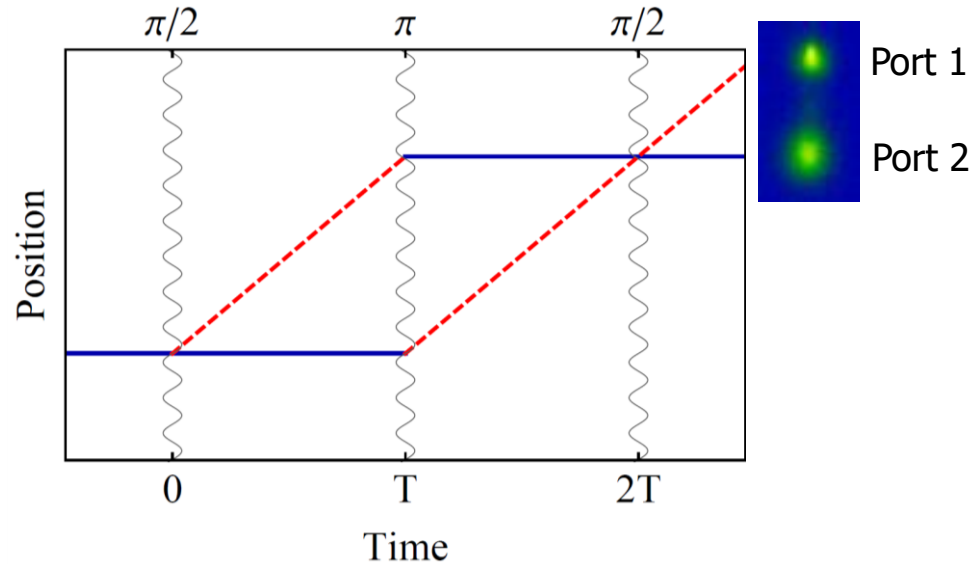
- General relativistic phase shift theory
- GR effects and clock interferometry
- Gravitational wave detection and MAGIS
- Aharonov-Bohm phase shifts
- **Tutorial:** Gravitational wave phase response

Lecture 3

- Advanced atom optics (large momentum transfer techniques)
- Systematic errors, backgrounds, and mitigations
- Supporting tools: matter wave lensing, optical lattices, phase shear readout

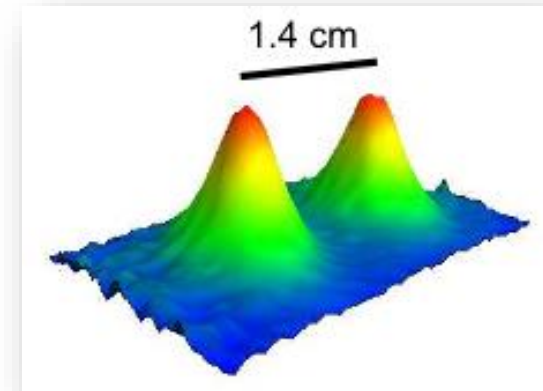
Lecture 2

Interference at long interrogation time



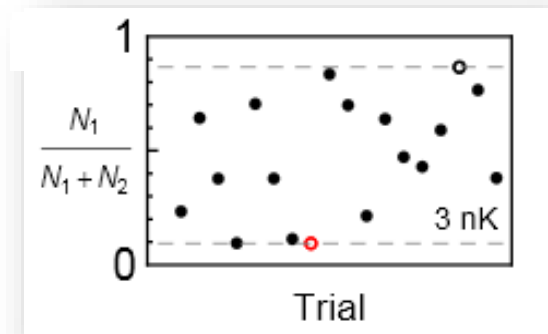
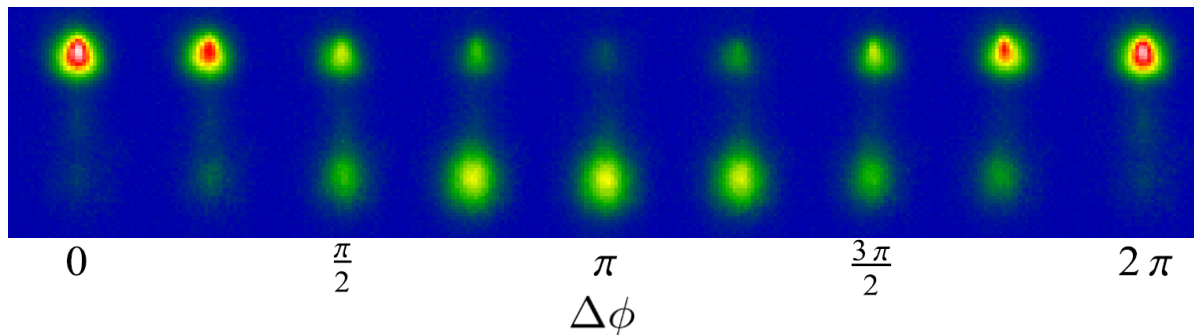
$2T = 2.3$ seconds

1.4 cm wavepacket separation



Wavepacket separation at apex (this data 50 nK)

Interference (3 nK cloud)

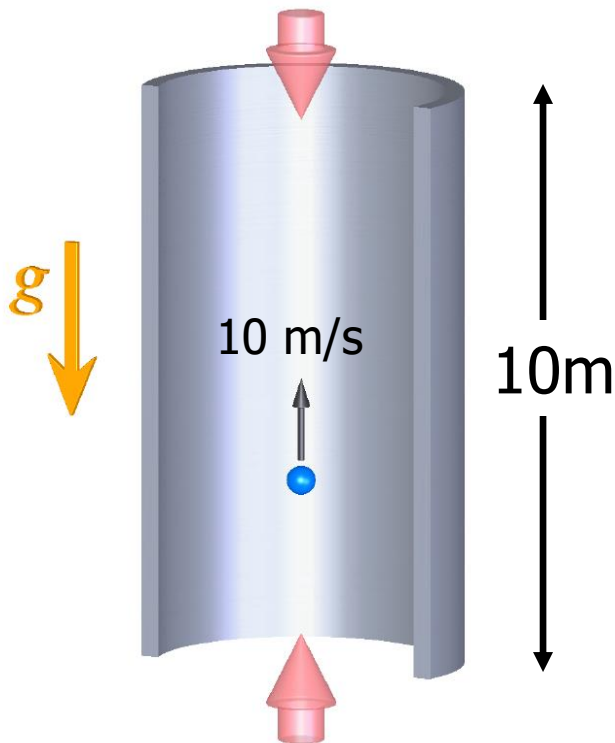


GR Back of the Envelope

Phase resolution target of some proposed experiments:

$$\frac{\delta\phi}{\phi} \approx 10^{-15}$$

At this level of sensitivity, does relativity start to affect results?



- Gravitational red shift of light:

$$\frac{\delta\nu}{\nu} = \frac{gL}{c^2} \approx 10^{-15}$$

- Special relativistic corrections:

$$\frac{v^2}{c^2} \approx 10^{-15}$$

Summary: Non-relativistic phase shift calculation

The atom interferometer phase shift can be decomposed as

$$\Delta\phi_{\text{tot}} = \Delta\phi_{\text{propagation}} + \Delta\phi_{\text{separation}} + \Delta\phi_{\text{laser}}$$

$$\Delta\phi_{\text{propagation}} = \sum_{\text{upper}} \left(\int_{t_I}^{t_F} (L_c - E_i) dt \right) - \sum_{\text{lower}} \left(\int_{t_I}^{t_F} (L_c - E_i) dt \right)$$

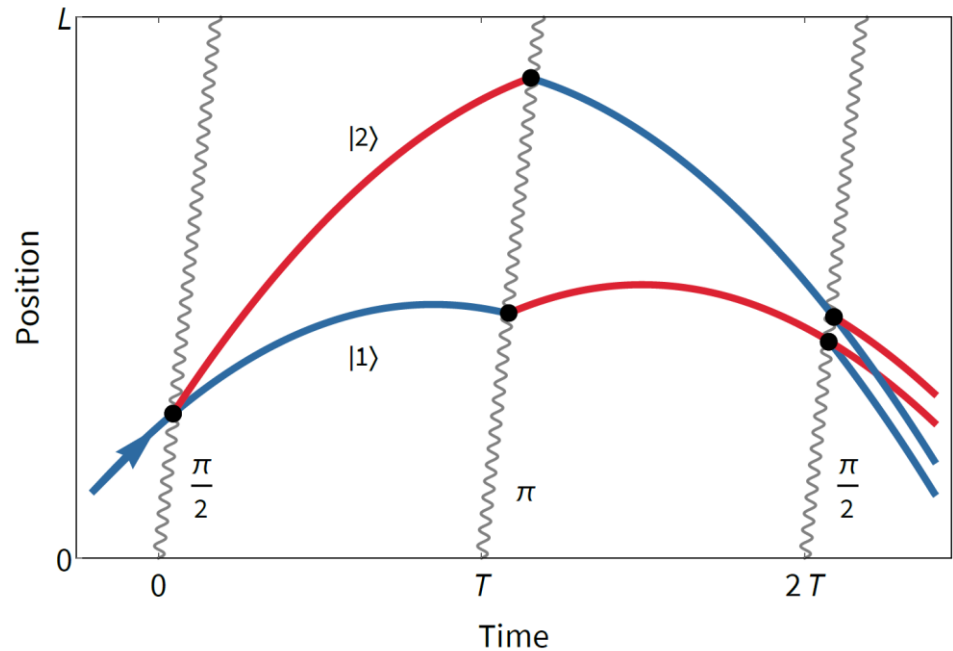
$$\Delta\phi_{\text{laser}} = \left(\sum_j \pm \phi_L(t_j, \mathbf{x}_u(t_j)) \right)_{\text{upper}} - \left(\sum_j \pm \phi_L(t_j, \mathbf{x}_l(t_j)) \right)_{\text{lower}}$$

$$\Delta\phi_{\text{separation}} = \bar{\mathbf{p}} \cdot \Delta\mathbf{x}$$

General relativistic phase shifts

Light-pulse interferometer phase shifts in GR:

- Geodesic propagation for atoms and light.
- Path integral formulation to obtain quantum phases.
- Atom-field interaction at intersection of laser and atom geodesics.



Atom and photon geodesics

Prior work, de Broglie interferometry: Post-Newtonian effects of gravity on quantum interferometry, Shigeru Wajima, Masumi Kasai, Toshifumi Futamase, Phys. Rev. D, 55, 1997; Bordé, et al.

Propagation Phase: The Atom's Clock

The atom's propagation phase measures proper time.

- Feynman path integral propagator:

$$\sum_{\text{paths}} e^{iS/\hbar}$$

- The action is modified in GR:

$$S_{\text{NR}} = \int L dt \quad \longrightarrow \quad S_{\text{GR}} = \int mc^2 d\tau$$

Proper time

- Propagation phase for atom:

$$\Delta\phi_{\text{propagation}} = \frac{1}{\hbar} \int L dt = \int \omega_{\text{C}} d\tau$$

Compton frequency (Cs):

$$\begin{aligned} \omega_{\text{C}} &= mc^2/\hbar \\ &= 3.2 \times 10^{25} \text{ Hz} \end{aligned}$$

The action is proportional to the length of the world line (proper time).

$$\phi_{\text{propagation}} = \int L dt = \int_{(c=1)} m d\tau = \int p_{\mu} dx^{\mu} \quad \begin{aligned} p^{\mu} &\equiv m \frac{dx^{\mu}}{d\tau} & d\tau^2 &= g_{\mu\nu} dx^{\mu} dx^{\nu} \\ p_{\mu} dx^{\mu} &= m g_{\mu\nu} \frac{dx^{\mu}}{d\tau} dx^{\nu} & &= m \frac{d\tau}{d\tau} d\tau \end{aligned}$$

Proper time, NR limit

Consider the proper time of a clock in the Schwarzschild spacetime:

$$ds^2 = (1 + 2\phi/c^2)c^2 dt^2 - \frac{1}{1 + 2\phi/c^2} dr^2 - r^2 d\Omega^2 \quad \phi(r) = -\frac{GM}{r} \approx -\frac{GM}{R_e} + gz$$

↖
Earth radius

Proper time: $c^2 d\tau^2 = g_{\mu\nu} dx^\mu dx^\nu$

$$c d\tau = \sqrt{g_{tt} + g_{rr} \frac{dr}{dt} \frac{dr}{dt}} dt$$

To first order in $\phi(r)$:

$$d\tau \approx \sqrt{1 + 2\phi(r)/c^2 - (v/c)^2} dt$$

$$\tau \approx \int \left(1 + \frac{\phi(r)}{c^2} - \frac{v^2}{2c^2} \right) dt$$

Gravitational redshift

Time dilation

Propagation Phase: Two Limits

$$S_{\text{GR}} = \int mc^2 d\tau$$

$$\Delta\phi_{\text{propagation}} = \frac{1}{\hbar} \int L dt = \int \omega_{\text{C}} d\tau$$

1. Non-relativistic limit:

$$S_{\text{GR}} = mc^2 \int \frac{d\tau}{dt} dt \approx mc^2 \int \left(1 + \frac{\phi(r)}{c^2} - \frac{v^2}{2c^2} \right) dt = \int (mc^2 + m\phi(r) - \frac{1}{2}mv^2) dt$$

(NR Lagrangian)

→ Proper time reduces to the non-relativistic Lagrangian.

2. Classical limit (Principle of Least Action):

→ QM: particles travel along the **extremal path** when $S \gg \hbar$

→ GR: particles travel along **geodesics**, paths that maximize proper time.

Atoms in an AI travel along the classical, geodesic path.

Atom-light interaction in LLF

Geodesic equation
$$\frac{d^2 x^\mu}{d\tau^2} + \Gamma_{\alpha\beta}^\mu \frac{dx^\alpha}{d\tau} \frac{dx^\beta}{d\tau} = 0$$

Local Lorentz Frame (LLF) is the freely-falling frame;
Christoffels transformed to zero



$$g_{\mu'\nu'}(x') = \eta_{\mu'\nu'} + \mathcal{O}(x'^2)$$

Metric *locally flat* in LLF

The atomic physics dynamics in the LLF are the *normal rules of non-relativistic quantum mechanics*. For example, the photon recoil is

$$m_{\text{in}} \frac{dx'^i_{\text{atom}}}{d\tau} \Big|_{\text{after}} = \underbrace{m_{\text{fi}} \frac{dx'^i_{\text{atom}}}{d\tau} \Big|_{\text{before}}}_{\text{atom momentum}} + \underbrace{\frac{dx'^i_{\text{light}}}{d\lambda}}_{\text{photon momentum}} \quad (\text{in LLF})$$

$$m_{\text{in}} = m_{\text{fi}} \pm \omega_a$$

atom mass change (internal energy of excited state)

There are small corrections $\mathcal{O}(R)$ due to Riemann curvature R , but these can be safely neglected since the atom is small.

Which LLF? The atom's recoil velocity says there is no unique frame!
True, but corrections are small, $\mathcal{O}(v_r^2)$

Laser phase

$$\Delta\phi_{\text{laser}} = \left(\sum_j \pm\phi_L(t_j, \mathbf{x}_u(t_j)) \right)_{\text{upper}} - \left(\sum_j \pm\phi_L(t_j, \mathbf{x}_l(t_j)) \right)_{\text{lower}}$$

A null geodesic is a 'path of constant phase'

Light field in flat spacetime:

$$\mathbf{E} = \mathbf{E}_0 e^{i\phi(x,t)} \quad \phi(x,t) = kx - \omega t$$

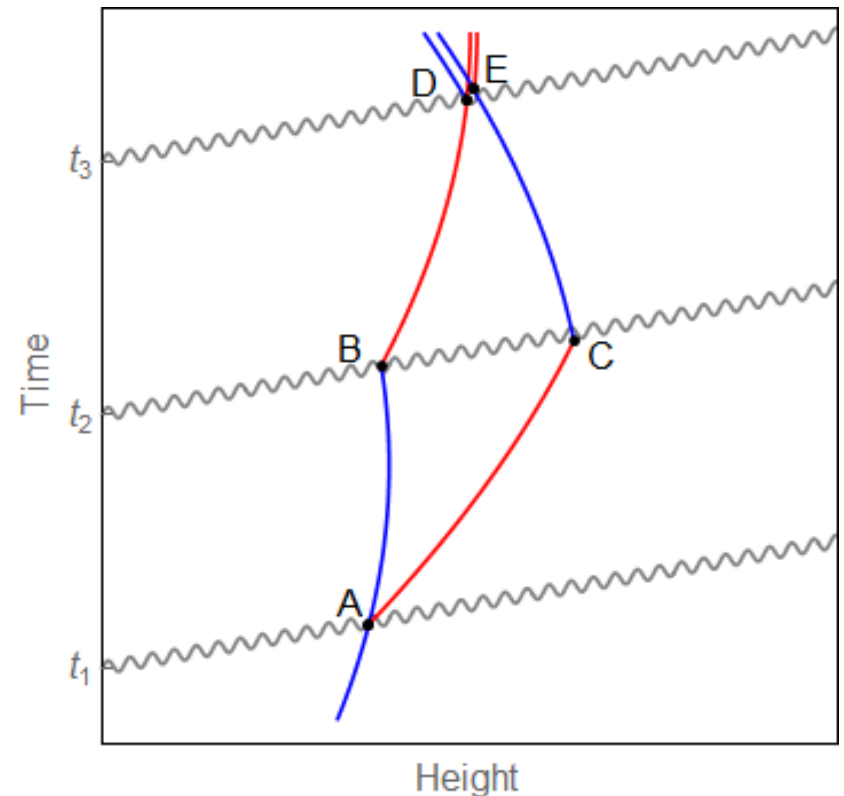
Path of constant phase is:

$$\phi(x,t) = \phi_0 = kx - \omega t$$

$$\rightarrow x(t) = ct + \frac{\phi_0}{k}$$

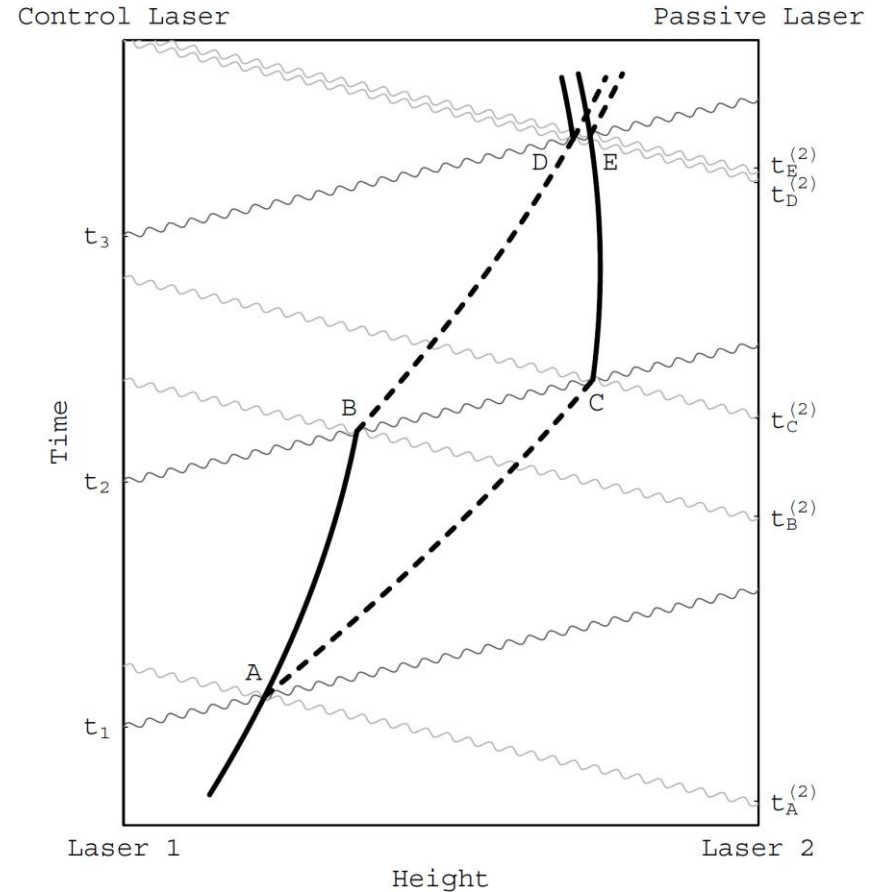
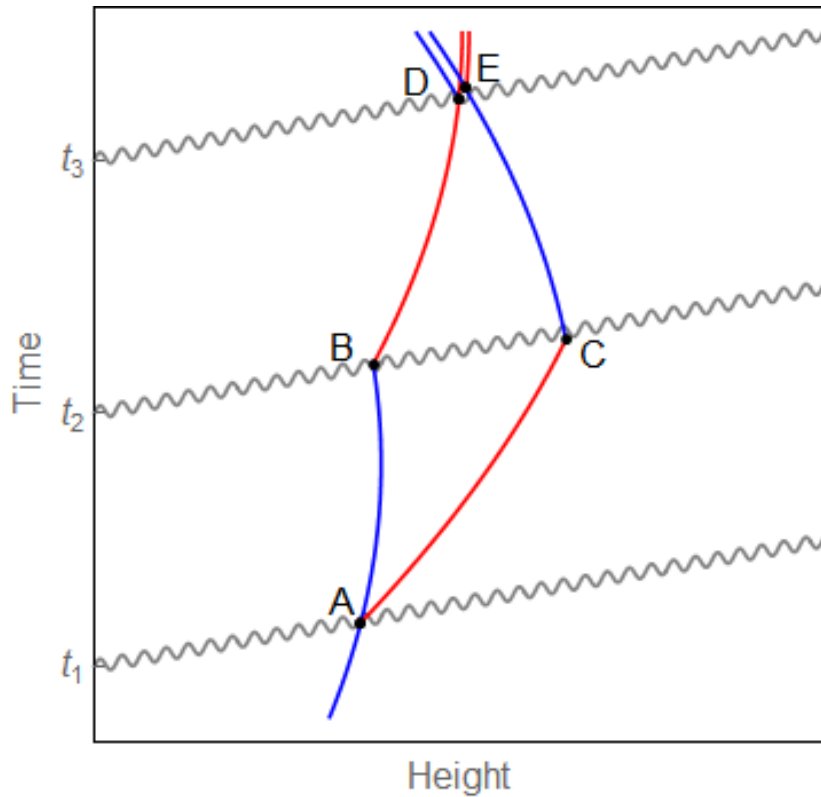
Generalize to curved space

$$\phi(x^\mu) = k_\mu x^\mu = g_{\mu\nu} k^\nu x^\mu = \phi_0$$



- Phase is **constant** along the null geodesic
- Phase imprinted on atom is the phase of light at (spacetime) point of emission

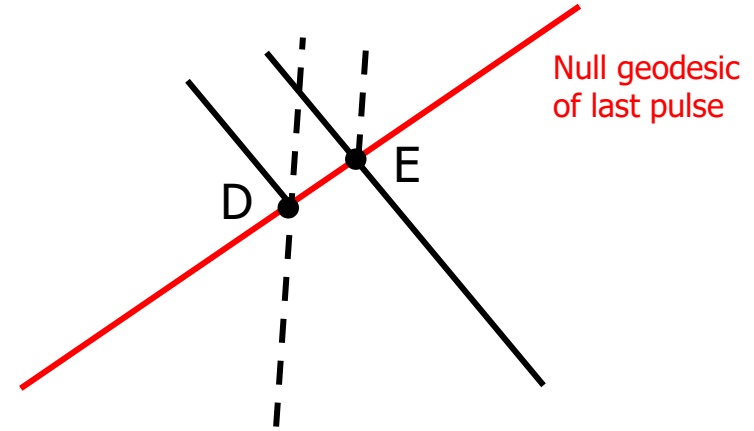
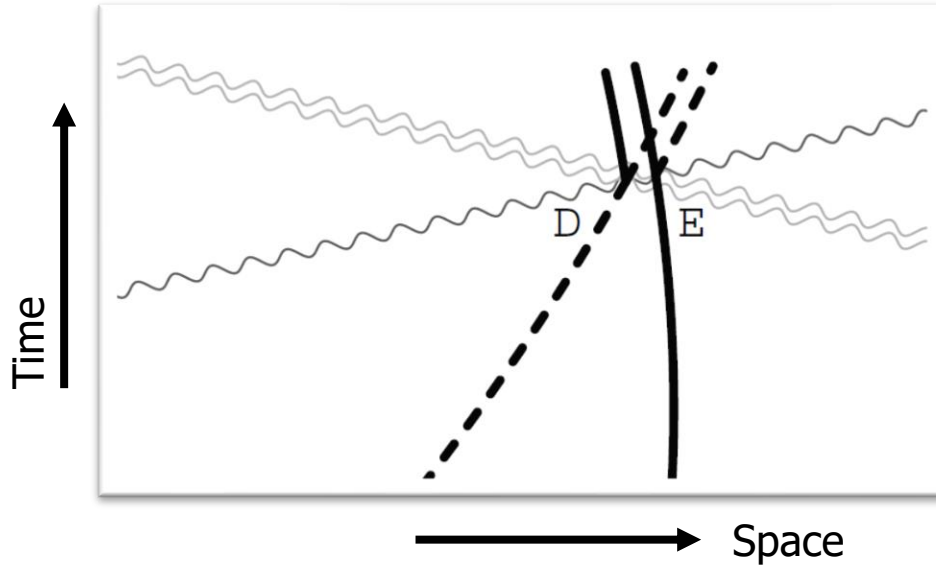
Single photon vs two photon atom optics



Consequential differences:

- For 2-photon, light pulses must leave at different times
- By convention, "passive" laser is on before "control" pulse arrives
- Arrival of control pulse determines passive null geodesic (and its laser phase)
- No passive laser for single photon atom optics

Separation phase



$$\bar{p}^\mu = \frac{1}{2} \left(m_o \frac{dx^\mu}{d\tau} \Big|_D + m_o \frac{dx^\mu}{d\tau} \Big|_E \right)$$

$$\Delta\phi_{\text{separation}} = \bar{\mathbf{p}} \cdot \Delta\mathbf{x} \quad \text{In the LLF} \rightarrow \quad \phi_{\text{separation}} = \int_E^D \bar{p}_{\mu'} dx'^{\mu'} \sim \bar{E} \Delta t' - \bar{\vec{p}} \cdot \Delta \vec{x}'$$

→ Phase to move from one wavepacket to the other in spacetime.

A very useful GR argument:

- The expression is the right answer in one frame (here, the LLF)
- It's written in a covariant manner
- Therefore, it's the correct relativistic result in all frames:

$$\phi_{\text{separation}} = \int_E^D \bar{p}_\mu dx^\mu \quad (\text{in any frame})$$

Example: Schwarzschild and PPN

Near the Earth,

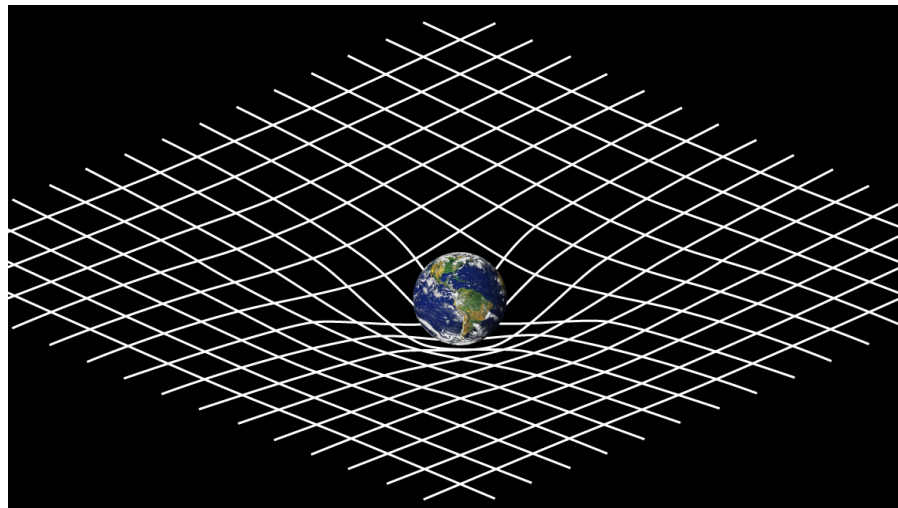
$$ds^2 = (1 + 2\phi) dt^2 - \frac{1}{1 + 2\phi} dr^2 - r^2 d\Omega^2 \quad \text{Schwarzschild}$$

$$\phi = -\frac{GM}{r} \quad \text{Very small } (\sim 1e-9)$$

$$ds^2 = (1 + 2\phi + 2\beta\phi^2) dt^2 - (1 - 2\gamma\phi) dr^2 - r^2 d\Omega^2 \quad \text{Parameterized post-Newtonian (PPN)}$$

β and γ parameters describe deviations from GR

$$\beta = \gamma = 1 \quad \text{in GR}$$



PPN geodesics are complicated

$$\begin{aligned}
 r(\tau) = & r_0 + v_{r0}\tau + \frac{(-v_{r0}^2(-1 + \gamma) + \eta + 2(v_{r0}^2(\beta - 2\gamma) + \beta\eta)\phi(r_0) - 6v_{r0}^2\beta\gamma\phi(r_0)^2)\partial_r\phi(r_0)}{2(-1 + 2\gamma\phi(r_0))(1 + 2\phi(r_0) + 2\beta\phi(r_0)^2)}\tau^2 + \\
 & \frac{1}{6}v_{r0}\left(\frac{2\gamma(v_{r0}^2(-1 + 2\gamma) - \eta - 2(v_{r0}^2(\beta - 3\gamma) + \beta\eta)\phi(r_0) + 8v_{r0}^2\beta\gamma\phi(r_0)^2)\partial_r\phi(r_0)^2}{(1 - 2\gamma\phi(r_0))^2(1 + 2\phi(r_0) + 2\beta\phi(r_0)^2)} + \right. \\
 & \left. \frac{2(-v_{r0}^2 - \eta + 2v_{r0}^2\gamma\phi(r_0))(-2 + \beta + \gamma - 6(\beta - \gamma)\phi(r_0) - 6\beta(\beta - 3\gamma)\phi(r_0)^2 + 16\beta^2\gamma\phi(r_0)^3)\partial_r\phi(r_0)^2}{(1 - 2\gamma\phi(r_0))^2(1 + 2\phi(r_0) + 2\beta\phi(r_0)^2)^2} + \right. \\
 & \left. \frac{v_{r0}^2\gamma\partial_r^2\phi(r_0)}{1 - 2\gamma\phi(r_0)} + \frac{(1 + 2\beta\phi(r_0))(v_{r0}^2 + \eta - 2v_{r0}^2\gamma\phi(r_0))\partial_r^2\phi(r_0)}{(-1 + 2\gamma\phi(r_0))(1 + 2\phi(r_0) + 2\beta\phi(r_0)^2)}\right)\tau^3 + \mathcal{O}(\tau^4)
 \end{aligned}$$

$$\begin{aligned}
 t(\tau) = & t_0 + \sqrt{\frac{v_{r0}^2 + \eta - 2v_{r0}^2\gamma\phi(r_0)}{1 + 2\phi(r_0) + 2\beta\phi(r_0)^2}}\tau - \frac{v_{r0}(1 + 2\beta\phi(r_0))\sqrt{\frac{v_{r0}^2 + \eta - 2v_{r0}^2\gamma\phi(r_0)}{1 + 2\phi(r_0) + 2\beta\phi(r_0)^2}}\partial_r\phi(r_0)}{1 + 2\phi(r_0) + 2\beta\phi(r_0)^2}\tau^2 - \\
 & \left(\left(\sqrt{\frac{v_{r0}^2 + \eta - 2v_{r0}^2\gamma\phi(r_0)}{1 + 2\phi(r_0) + 2\beta\phi(r_0)^2}}\left((-v_{r0}^2(-5 + 2\beta + \gamma) + \eta + 2(v_{r0}^2(-6\gamma + \beta(8 + \gamma)) + 2\beta\eta)\phi(r_0) + \right.\right.\right. \\
 & \left.\left.\left.2\beta(v_{r0}^2(8\beta - 19\gamma) + 2\beta\eta)\phi(r_0)^2 - 36v_{r0}^2\beta^2\gamma\phi(r_0)^3)\partial_r\phi(r_0)^2 + \right.\right.\right. \\
 & \left.\left.\left. v_{r0}^2(-1 + 2\gamma\phi(r_0))(1 + 2(1 + \beta)\phi(r_0) + 6\beta\phi(r_0)^2 + 4\beta^2\phi(r_0)^3)\partial_r^2\phi(r_0)\right)\right)\tau^3 / \right. \\
 & \left. \left(3\left((-1 + 2\gamma\phi(r_0))(1 + 2\phi(r_0) + 2\beta\phi(r_0)^2)^2\right)\right) + \mathcal{O}(\tau^4)
 \end{aligned}$$

Dimopoulos et al., PRD 78 (2008)

- This expression can be used for both the light and atom geodesics (choose η) $\eta = g_{\mu\nu}\frac{dx^\mu}{d\tau}\frac{dx^\nu}{d\tau}$
- Need to find intersection points!
- Can solve perturbatively (small velocity, weak gravity)
- Consistently Taylor expand in all small variables simultaneously: “physical series”

PPN phase shift results

	GR Phase Shift	Size (rad)	Interpretation	NR Phase Shift
1.	$-k_{\text{eff}}gT^2$	$3. \times 10^8$	Newtonian gravity	$-k_{\text{eff}}gT^2$
2.	$-k_{\text{eff}}(\partial_r g)v_L T^3$	$-2. \times 10^3$	1st gradient	$-k_{\text{eff}}(\partial_r g)v_L T^3$
3.	$-\frac{7}{12}k_{\text{eff}}(\partial_r g)gT^4$	$9. \times 10^2$		$-\frac{7}{12}k_{\text{eff}}(\partial_r g)gT^4$
4.	$-3k_{\text{eff}}g^2T^3$	$-4. \times 10^1$	finite speed of light and	
5.	$-3k_{\text{eff}}gv_L T^2$	$4. \times 10^1$	Doppler shift corrections	
6.	$-\frac{k_{\text{eff}}^2}{2m}(\partial_r g)T^3$	$-7. \times 10^{-1}$	1st gradient recoil	$-\frac{k_{\text{eff}}^2}{2m}(\partial_r g)T^3$
7.	$(\omega_{\text{eff}} - \omega_a)gT^2$	$-4. \times 10^{-1}$	detuning	
8.	$(2 - 2\beta - \gamma)k_{\text{eff}}g\phi T^2$	$-2. \times 10^{-1}$	GR (non-linearity)	
9.	$-\frac{3k_{\text{eff}}^2}{2m}gT^2$	$2. \times 10^{-2}$		
10.	$-\frac{7}{12}k_{\text{eff}}v_L^2(\partial_r^2 g)T^4$	$8. \times 10^{-3}$	2nd gradient	$-\frac{7}{12}k_{\text{eff}}v_L^2(\partial_r^2 g)T^4$
11.	$-\frac{35}{4}k_{\text{eff}}(\partial_r g)gv_L T^4$	$6. \times 10^{-4}$		
12.	$-4k_{\text{eff}}(\partial_r g)v_L^2 T^3$	$-3. \times 10^{-4}$		
13.	$2\omega_a g^2 T^3$	$2. \times 10^{-4}$		
14.	$2\omega_a gv_L T^2$	$-2. \times 10^{-4}$		
15.	$-\frac{7k_{\text{eff}}^2}{12m}v_L(\partial_r^2 g)T^4$	$7. \times 10^{-6}$	2nd gradient recoil	$-\frac{7k_{\text{eff}}^2}{12m}v_L(\partial_r^2 g)T^4$
16.	$-12k_{\text{eff}}g^2v_L T^3$	$-7. \times 10^{-6}$		
17.	$-7k_{\text{eff}}g^3 T^4$	$4. \times 10^{-6}$		
18.	$-5k_{\text{eff}}gv_L^2 T^2$	$3. \times 10^{-6}$	GR (velocity-dependent force)	
19.	$(2 - 2\beta - \gamma)k_{\text{eff}}\partial_r(g\phi)v_L T^3$	$2. \times 10^{-6}$	GR 1st gradient	
20.	$\frac{7}{12}(4 - 4\beta - 3\gamma)k_{\text{eff}}\phi(\partial_r g)gT^4$	$-2. \times 10^{-6}$	GR	
21.	$(\omega_{\text{eff}} - \omega_a)(\partial_r g)v_L T^3$	$2. \times 10^{-6}$		
22.	$\frac{7}{12}(\omega_{\text{eff}} - \omega_a)(\partial_r g)gT^4$	$-1. \times 10^{-6}$		
23.	$-\frac{7}{12}(2 - 2\beta - \gamma)k_{\text{eff}}g^3 T^4$	$-3. \times 10^{-7}$	GR	
24.	$-\frac{7k_{\text{eff}}^2}{2m_0}(\partial_r g)v_L T^3$	$-2. \times 10^{-7}$		
25.	$-\frac{27k_{\text{eff}}^2}{8m}(\partial_r g)gT^4$	$2. \times 10^{-7}$		
26.	$\frac{k_{\text{eff}}\omega_a}{m}gT^2$	$-1. \times 10^{-7}$		
27.	$6(2 - 2\beta - \gamma)k_{\text{eff}}\phi g^2 T^3$	$5. \times 10^{-8}$	GR	
28.	$3(\omega_{\text{eff}} - \omega_a)g^2 T^3$	$4. \times 10^{-8}$		
29.	$3(\omega_{\text{eff}} - \omega_a)gv_L T^2$	$-4. \times 10^{-8}$		
30.	$6(1 - \beta)k_{\text{eff}}\phi gv_L T^2$	$3. \times 10^{-8}$	GR	

Missing from NR calc

“not previously known because their calculation requires a fully relativistic calculation”

Clock AI response

Single photon vs. two photon AI

Breakdown the origin of various phase terms in the relativistic calculation (for Raman transitions)

	Parameter dependence	Total phase shift coefficient	Propagation phase coefficient	Separation phase coefficient	Laser phase coefficient	Size (rad)
1.	$k_{\text{eff}}T^3(\partial_r g)$	0	1	-1	0	4×10^{10}
2.	$k_{\text{eff}}gT^2$	-1	-1	1	-1	3×10^8
3.	$\omega_{\text{eff}}gT^2$	1	2	-2	1	3×10^3
4.	$\omega_a g T^2$	-1	-1	0	0	3×10^3
5.	$k_{\text{eff}}(\partial_r g)T^3 v_L$	-1	2	-2	-1	2×10^3
6.	$k_{\text{eff}}(\partial_r g)\phi T^3$	0	$2\gamma + 2\beta - 2$	$-2\gamma - 2\beta + 2$	0	3×10^1
7.	$k_{\text{eff}}gT^2 v_L$	-3	-5	5	-3	1×10^1
8.	$k_{\text{eff}}g\phi T^2$	$2 - 2\beta - \gamma$	$2 - 2\beta - \gamma$	$-2 + 2\beta + \gamma$	$2 - 2\beta - \gamma$	2×10^{-1}
9.	$k_{\text{eff}}g^2 T^3 v_L$	-12	-17	17	-12	7×10^{-6}
10.	$k_{\text{eff}}\partial_r(g\phi)T^3 v_L$	$2 - 2\beta - \gamma$	$-4 + 4\beta + 2\gamma$	$4 - 4\beta - 2\gamma$	$2 - 2\beta - \gamma$	2×10^{-6}
11.	$k_{\text{eff}}gT^2 v_L^2$	-5	-9	9	-5	5×10^{-7}

- GR calculation gives terms arising from **change of rest mass** in different atomic states.
- In the case of a single photon interferometer, this is the dominate effect.
- Phase shift comes from propagation phase, not laser phase.
- Leading single photon AI phase shift **does not depend on the laser wavevector**.
- Non-relativistic single photon calculation incorrectly predicts kgT^2

General Relativity Effects

Schwarzschild metric, PPN expansion:

$$ds^2 = (1 + 2\phi + 2\beta\phi^2)dt^2 - (1 - 2\gamma\phi)dr^2 - r^2d\Omega^2$$

$$\frac{d\vec{v}}{dt} = -\vec{\nabla}[\phi + (\beta + \gamma)\phi^2] + \gamma[3(\vec{v} \cdot \hat{r})^2 - 2\vec{v}^2]\vec{\nabla}\phi + 2\vec{v}(\vec{v} \cdot \vec{\nabla}\phi).$$

Coordinate
acceleration, from
geodesic equation

↑
Newtonian
Gravity

↑
Gravity
Gravitates

↑ ↑
Kinetic Energy
Gravitates

Corresponding AI phase shifts:

	Phase Shift	Size (rad)	Interpretation
1.	$-k_{\text{eff}}gT^2$	3×10^8	gravity
2.	$-k_{\text{eff}}(\partial_r g)T^3 v_L$	-2×10^3	1st gradient
3.	$-3k_{\text{eff}}gT^2 v_L$	4×10^1	Doppler shift
4.	$(2 - 2\beta - \gamma)k_{\text{eff}}g\phi T^2$	2×10^{-1}	GR
5.	$-\frac{7}{12}k_{\text{eff}}(\partial_r^2 g)T^4 v_L^2$	8×10^{-3}	2nd gradient
6.	$-5k_{\text{eff}}gT^2 v_L^2$	3×10^{-6}	GR
7.	$(2 - 2\beta - \gamma)k_{\text{eff}}\partial_r(g\phi)T^3 v_L$	2×10^{-6}	GR 1st grad
8.	$-12k_{\text{eff}}g^2 T^3 v_L$	-6×10^{-7}	GR

Projected experimental limits:

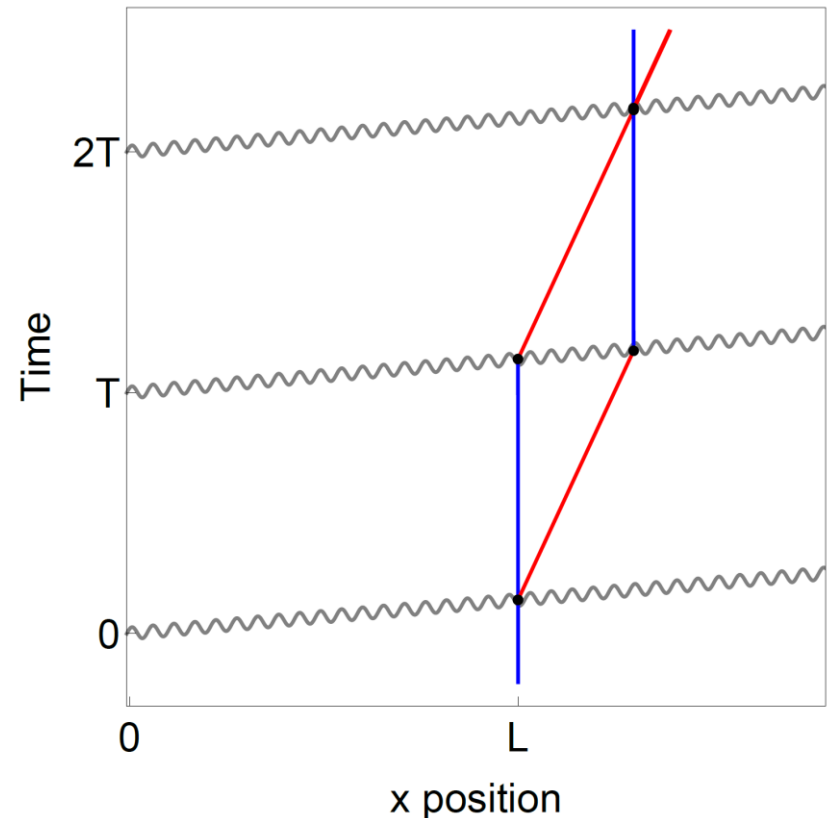
Tested Effect	current limit	AI initial	AI upgrade	AI future	AI far future
PoE	3×10^{-13}	10^{-15}	10^{-16}	10^{-17}	10^{-19}
PPN (β, γ)	10^{-4} - 10^{-5}	10^{-1}	10^{-2}	10^{-4}	10^{-6}

Example: Gravitational waves

Metric in TT gauge

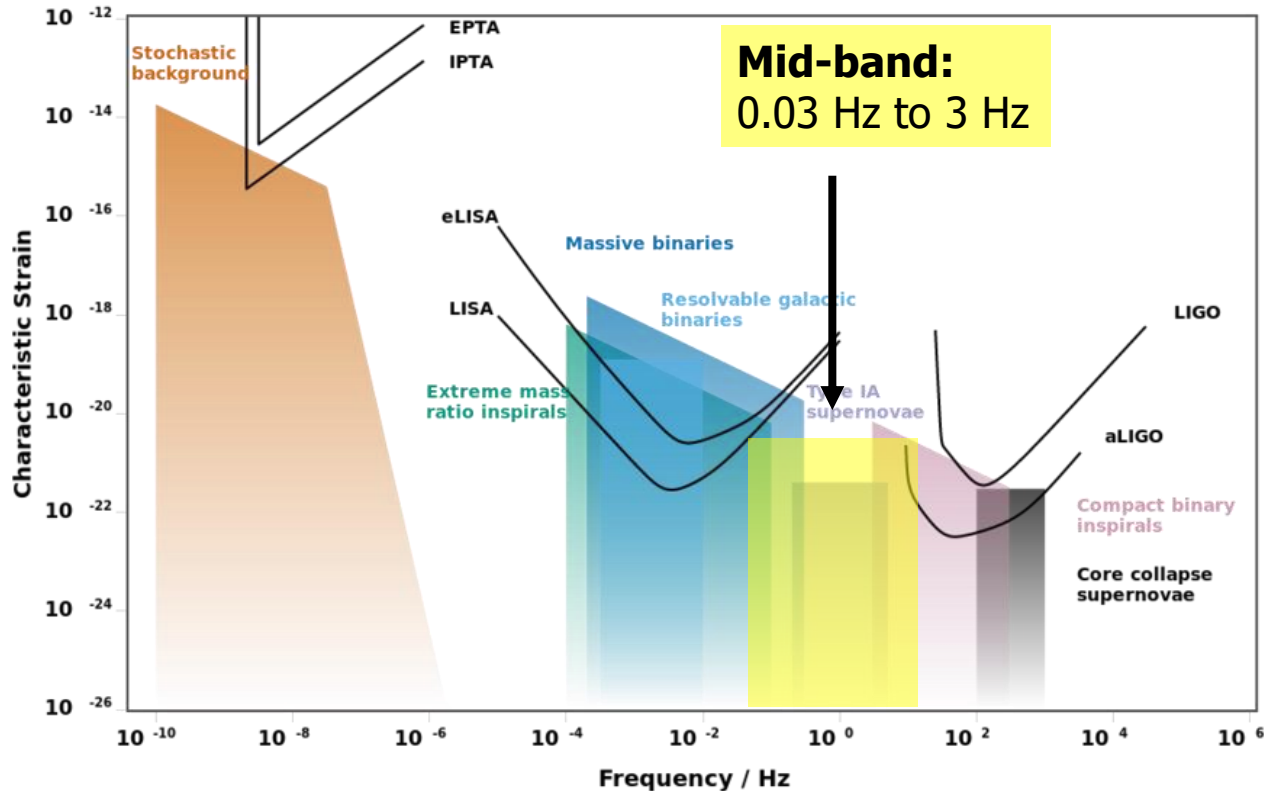
$$ds^2 = dt^2 - (1 + h \sin(\omega(t - z)))dx^2 - (1 - h \sin(\omega(t - z)))dy^2 - dz^2$$

- Geodesics much simpler, since h is small
- For MAGIS-like configurations, can ignore motion of atom (recoil effects are corrections)
- GW signal arises from affect on null geodesics (in TT gauge)
- Arrival time of light determines atom propagation phase ('clock' phase)
- Laser phase is suppressed in a gradiometer configuration



Atomic sensors for gravitational wave detection

Atomic clocks and **atom interferometry** offer the potential for gravitational wave detection in an *unexplored frequency range* ("mid-band")



Mid-band science

- LIGO sources before they reach LIGO band
- Sky localization: predict when and where events will occur (multi-messenger astronomy)
- Cosmological sources
- Wave-like dark matter (dilaton, ALP, ...)

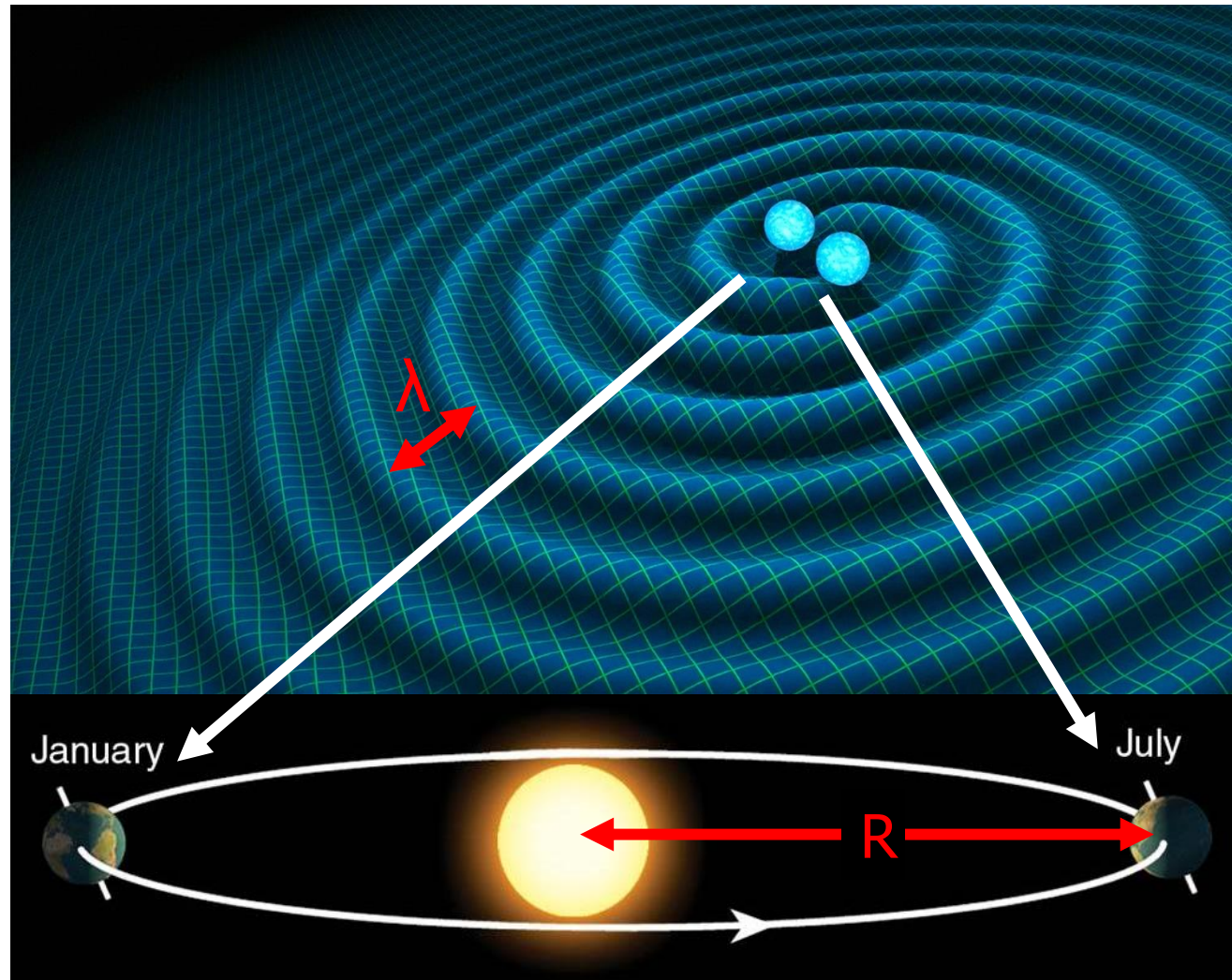
Sky position determination

Sky localization
precision:

$$\sqrt{\Omega_s} \sim \left(\text{SNR} \cdot \frac{R}{\lambda} \right)^{-1}$$

Mid-band advantages

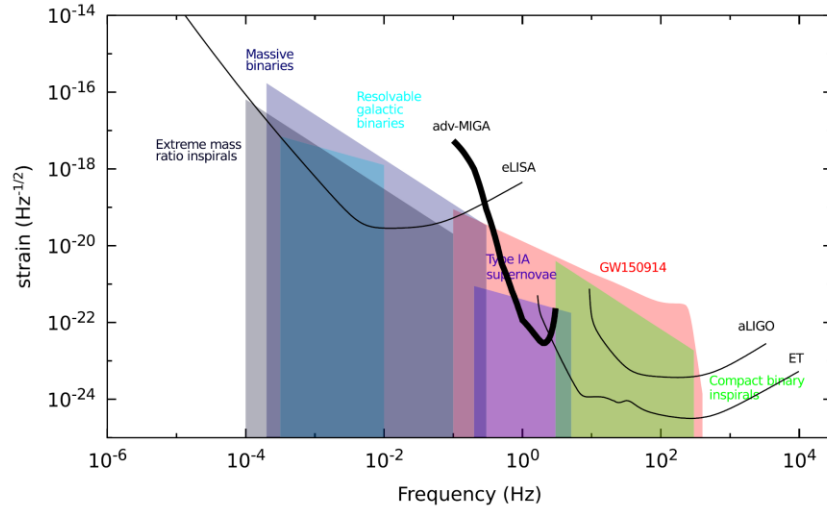
- Small wavelength λ
- Long source lifetime (\sim months) maximizes effective R



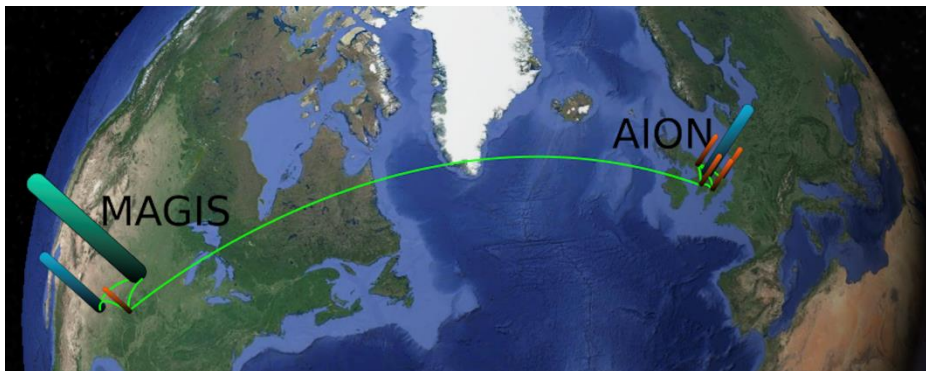
Benchmark	$\sqrt{\Omega_s}$ [deg]
GW150914	0.16
GW151226	0.20
NS-NS (140 Mpc)	0.19

International efforts in atomic sensors for mid-band GW

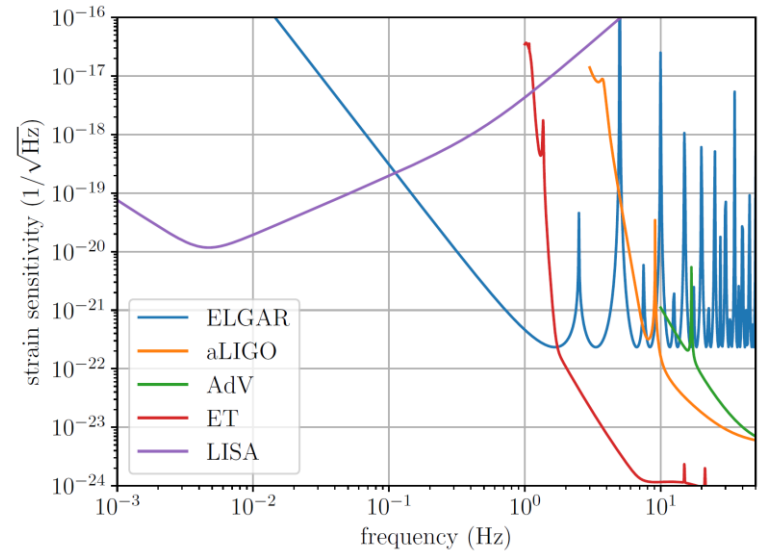
MIGA: Matter Wave laser Interferometric Gravitation Antenna (France)



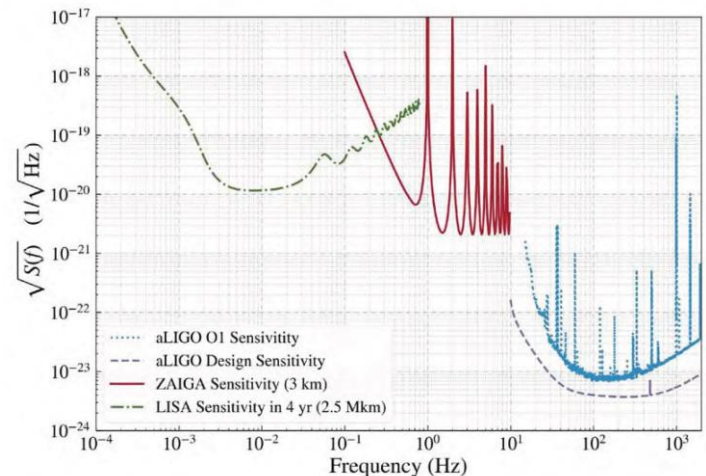
AION: Atom Interferometer Observatory and Network (UK)



ELGAR: European Laboratory for Gravitation and Atom-interferometric Research

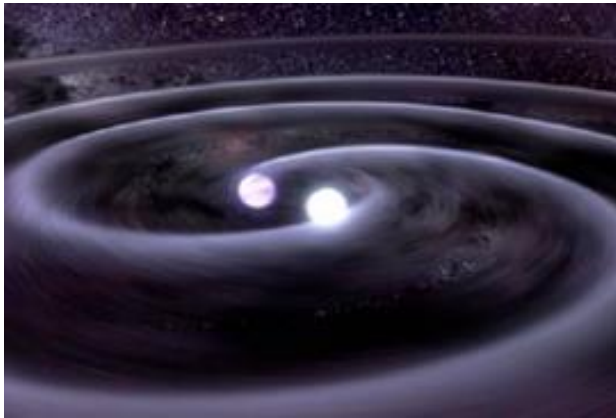


ZAIGA: Zhaoshan Long-baseline Atom Interferometer Gravitation Antenna (China)

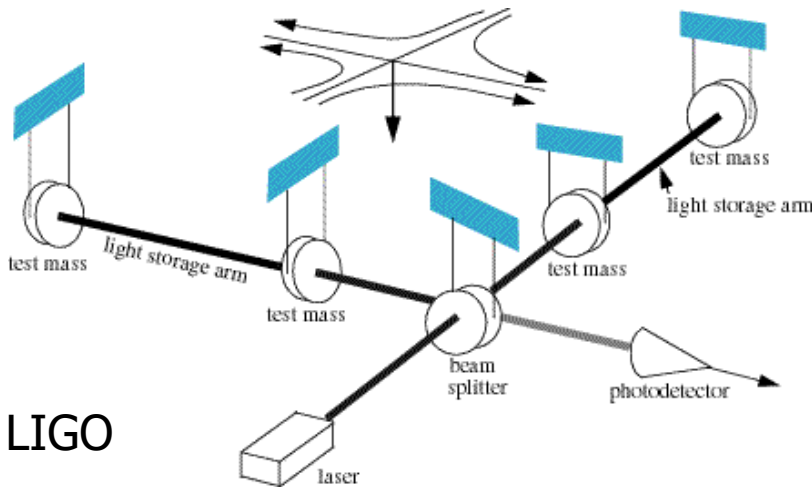
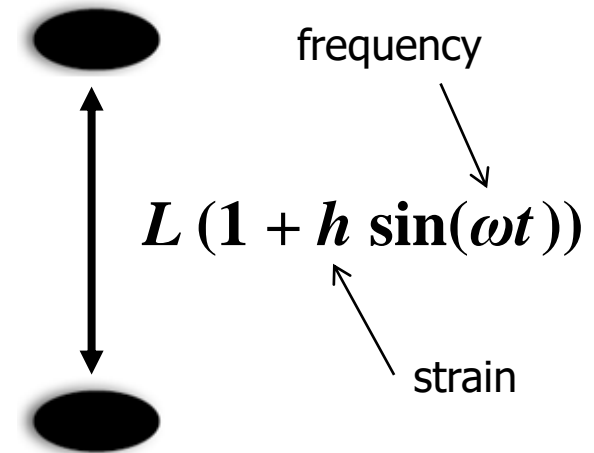


Gravitational Wave Detection

$$ds^2 = dt^2 - (1 + h \sin(\omega(t - z)))dx^2 - (1 - h \sin(\omega(t - z)))dy^2 - dz^2$$



Megaparsecs...



LIGO

- LIGO and other optical interferometers **use two baselines**
- In principle, **only one is required**
- Second baseline needed to reject laser technical noise

MAGIS concept

Matter wave **A**tomic **G**radiometer **I**nterferometric **S**ensor

Passing gravitational waves cause a small modulation in the distance between objects.

Detecting this modulation requires two ingredients:

1. Inertial references

- Freely-falling objects, separated by some baseline
- Must be insensitive to perturbations from non-gravitational forces

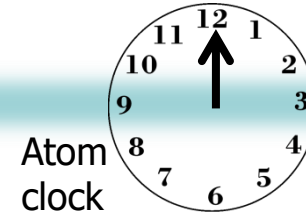
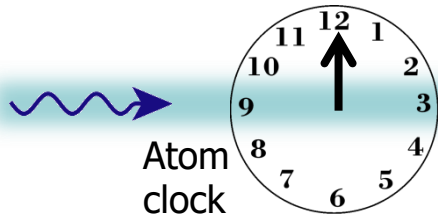
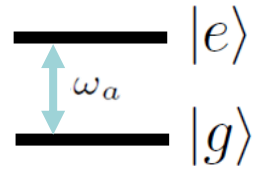
2. Clock

- Used to monitor the separation between the inertial references
- Typically measures the time for light to cross the baseline, via comparison to a precise phase reference (e.g. a clock).

In MAGIS, atoms play both roles.

Atom as “active” proof mass: Atomic coherence records laser phase, avoiding the need of a reference baseline – **single baseline** gravitational wave detector.

Simple Example: Two Atomic Clocks



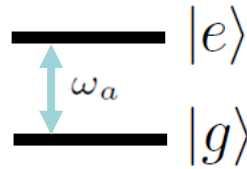
Phase evolved by atom after time T

$$\frac{1}{\sqrt{2}} |g\rangle + \frac{1}{\sqrt{2}} |e\rangle e^{-i\omega_a T}$$

$$\frac{1}{\sqrt{2}} |g\rangle + \frac{1}{\sqrt{2}} |e\rangle e^{-i\omega_a T}$$

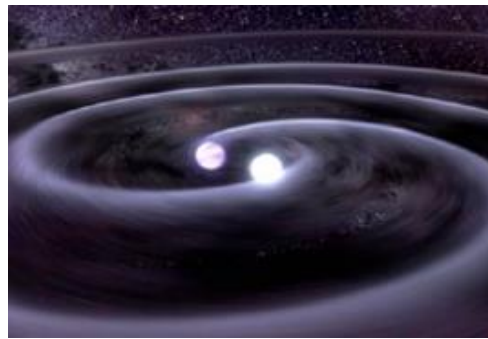
Time

Simple Example: Two Atomic Clocks



$$\frac{1}{\sqrt{2}} |g\rangle + \frac{1}{\sqrt{2}} |e\rangle$$

$$\frac{1}{\sqrt{2}} |g\rangle + \frac{1}{\sqrt{2}} |e\rangle$$



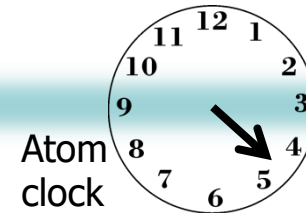
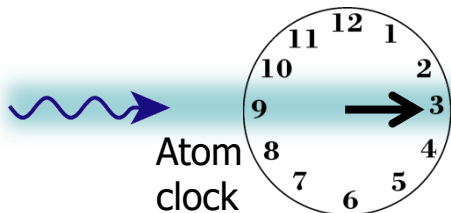
GW changes light travel time

$$\Delta T \sim hL/c$$

Time

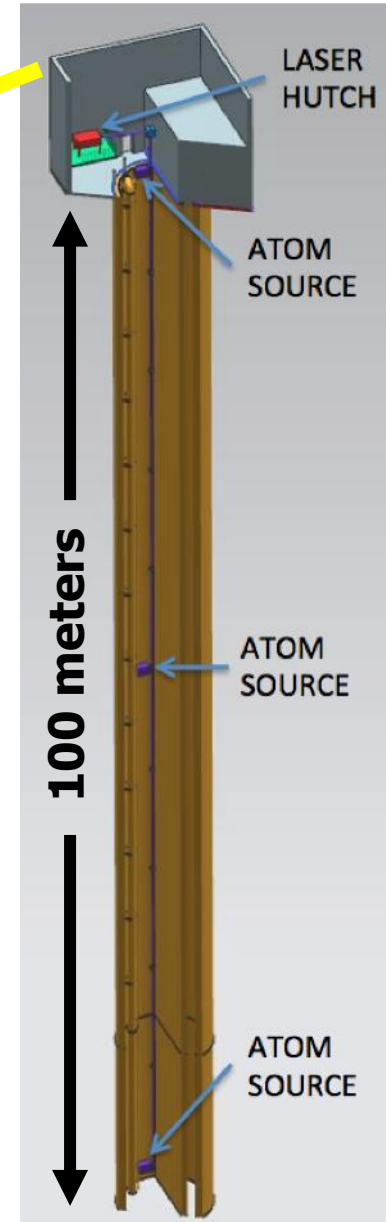
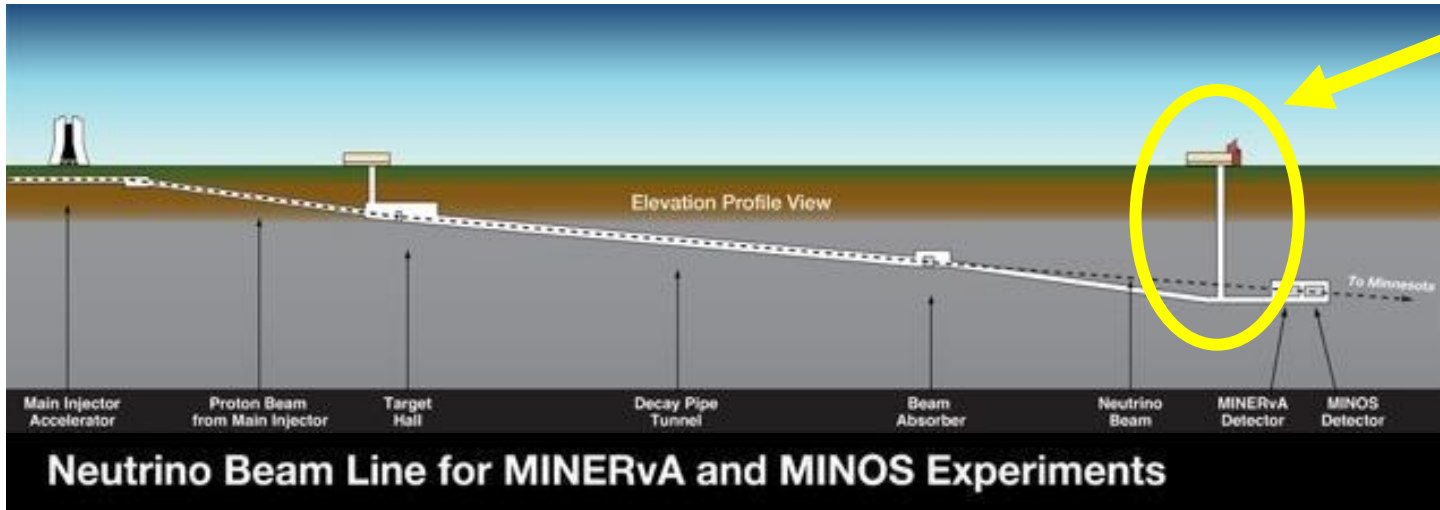
$$\frac{1}{\sqrt{2}} |g\rangle + \frac{1}{\sqrt{2}} |e\rangle e^{-i\omega_a T}$$

$$\frac{1}{\sqrt{2}} |g\rangle + \frac{1}{\sqrt{2}} |e\rangle e^{-i\omega_a (T + \Delta T)}$$



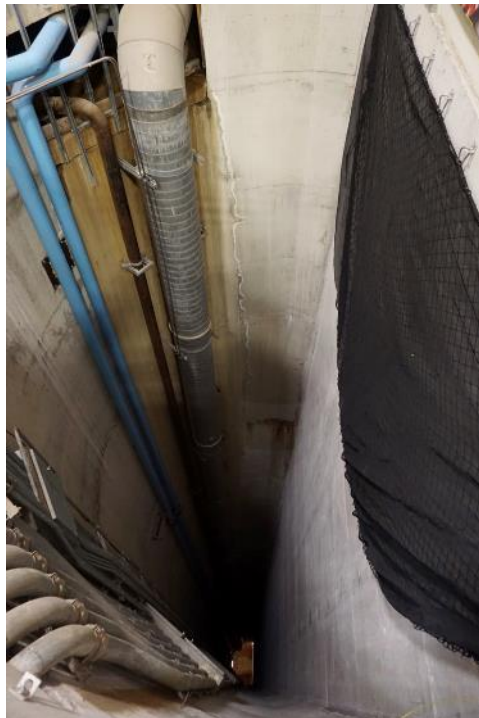
MAGIS-100: Detector prototype at Fermilab

Matter wave **A**tomic **G**radiometer **I**nterferometric **S**ensor



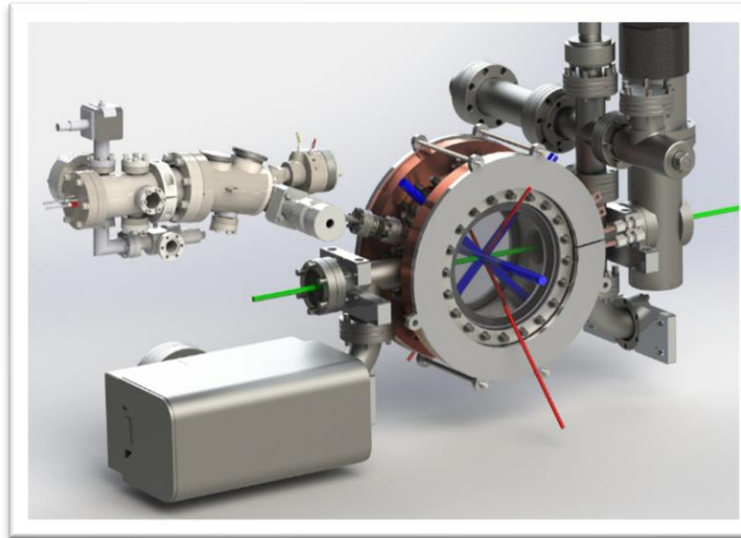
- 100-meter baseline atom interferometry in existing shaft at Fermilab
- Intermediate step to full-scale (km) detector for gravitational waves
- Clock atom sources (Sr) at three positions to realize a gradiometer
- Probes for ultralight scalar dark matter beyond current limits (Hz range)
- Extreme quantum superposition states: >meter wavepacket separation, up to 9 seconds duration

MAGIS-100 design

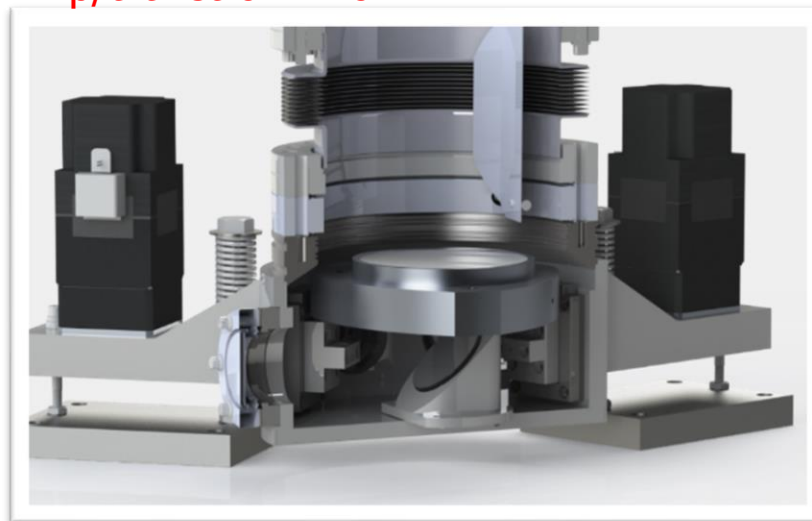


Minos access shaft

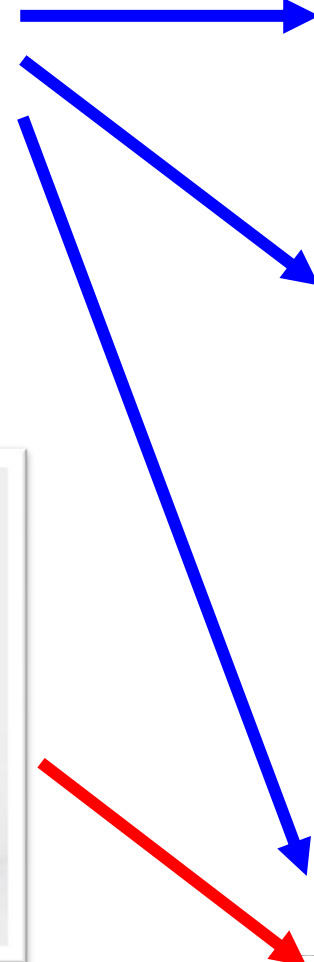
Interferometer laser system



Tip/tilt retro mirror



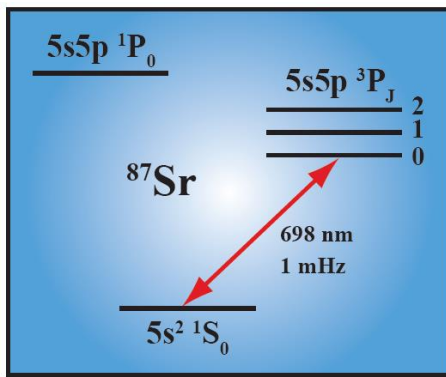
Sr atom sources



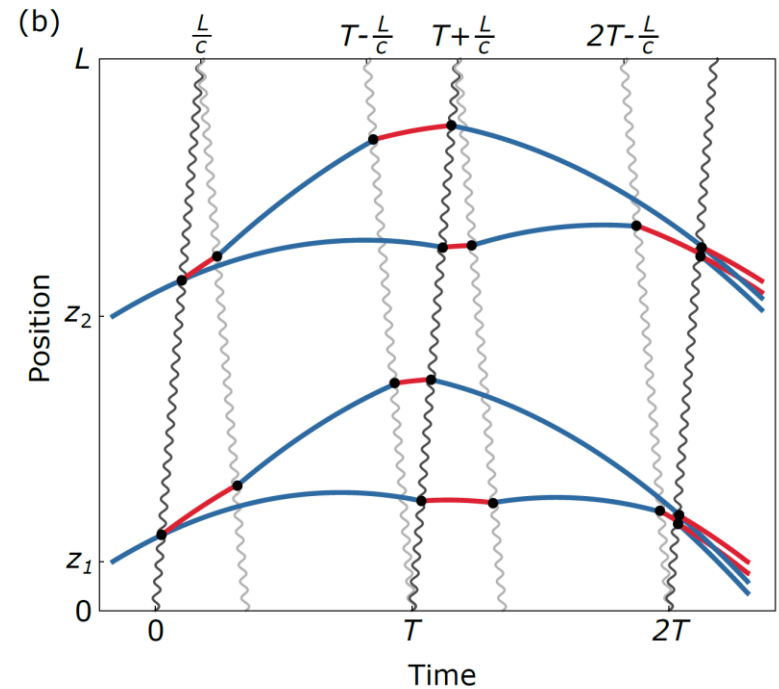
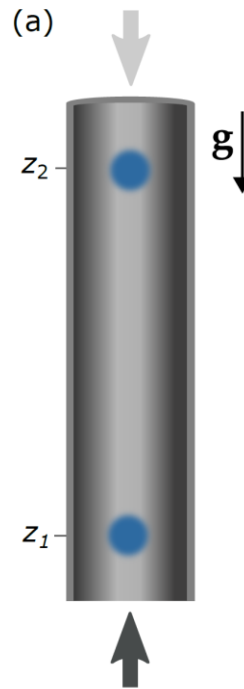
100 meters

Clock atom interferometry

New kind of atom interferometry using **single-photon transitions** between long-lived **clock states**



Clock transition in candidate atom ^{87}Sr



Excited state phase evolution:

$$\Delta\phi \sim \omega_A (2L/c)$$

(variations over time T)

Two ways for phase to vary:

$$\delta\omega_A \quad \text{Dark matter}$$

$$\delta L = hL \quad \text{Gravitational wave}$$

Graham et al., PRL **110**, 171102 (2013).

Arvanitaki et al., PRD **97**, 075020 (2018).

Ultralight (wave-like) dark matter

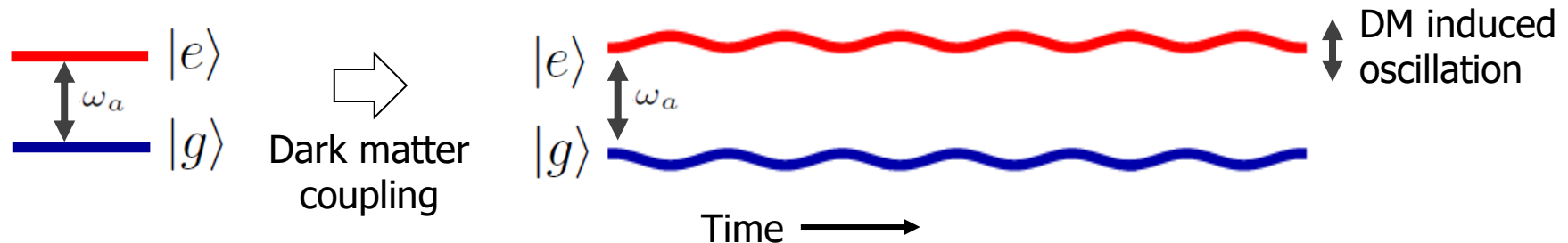
Ultralight dilaton DM acts as a background field (e.g., mass $\sim 10^{-15}$ eV)

$$\mathcal{L} = + \frac{1}{2} \partial_\mu \phi \partial^\mu \phi - \frac{1}{2} m_\phi^2 \phi^2 - \sqrt{4\pi G_N} \phi \left[\underbrace{d_{m_e} m_e \bar{e} e}_{\text{Electron coupling}} - \frac{d_e}{4} \underbrace{F_{\mu\nu} F^{\mu\nu}}_{\text{Photon coupling}} \right] + \dots$$

↓ DM scalar field

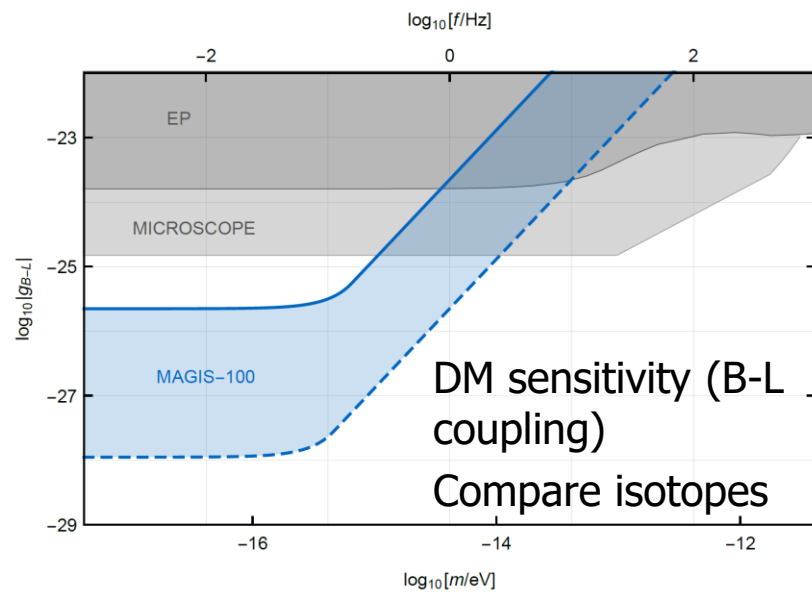
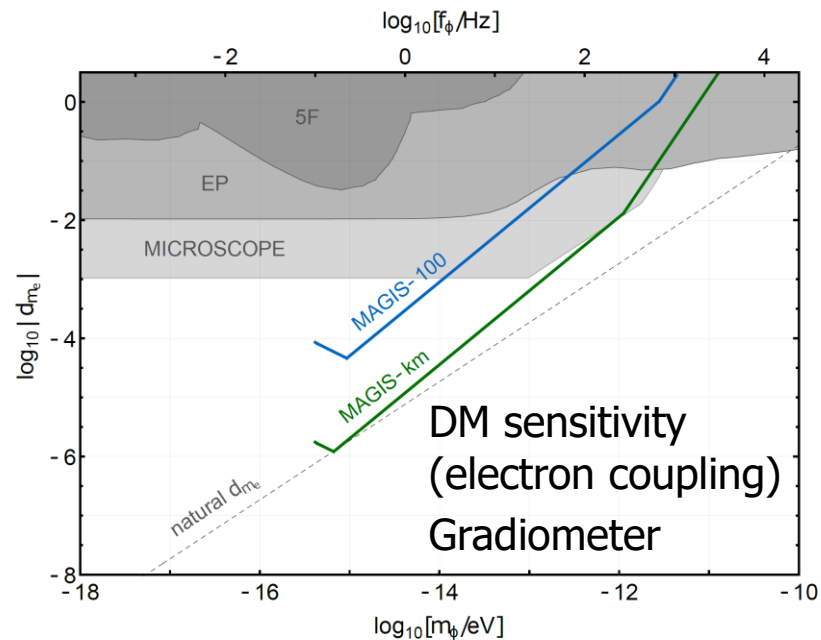
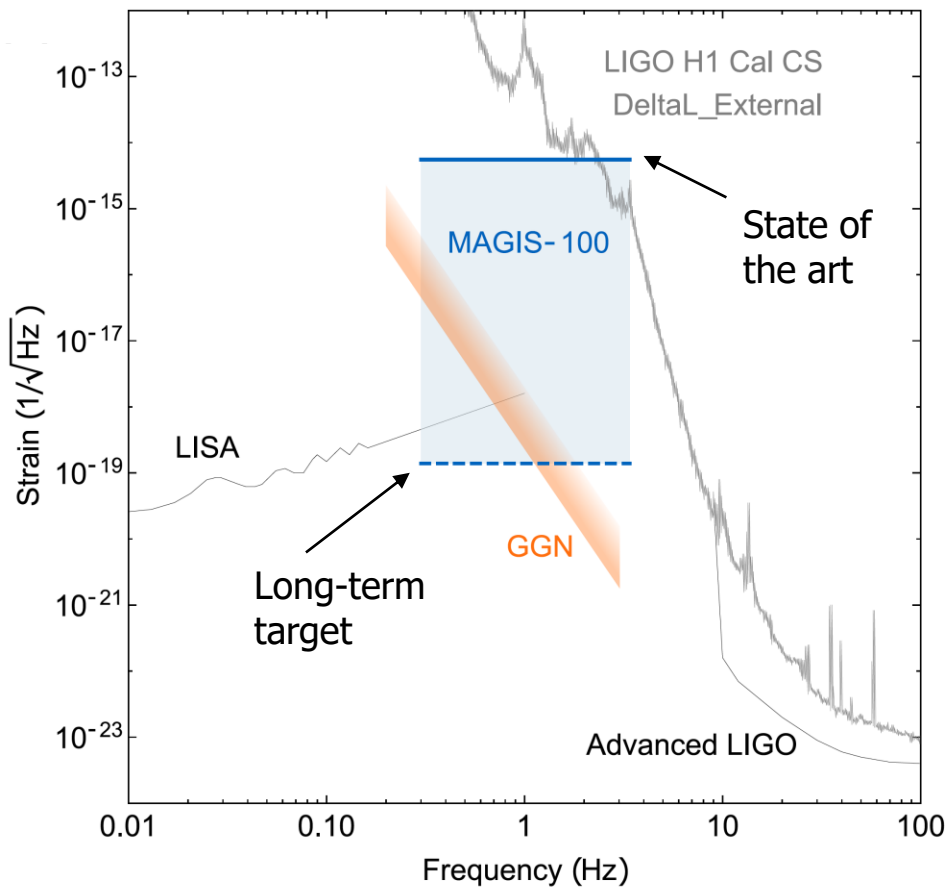
$$\phi(t, \mathbf{x}) = \phi_0 \cos [m_\phi(t - \mathbf{v} \cdot \mathbf{x}) + \beta] + \mathcal{O}(|\mathbf{v}|^2) \quad \phi_0 \propto \sqrt{\rho_{\text{DM}}} \quad \text{DM mass density}$$

DM coupling causes time-varying atomic energy levels:

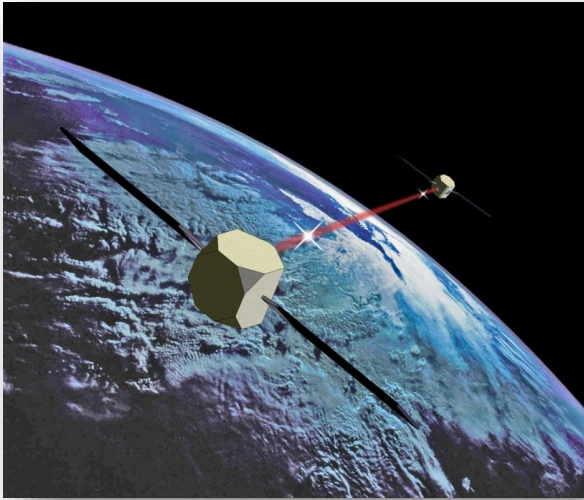


MAGIS-100 projected sensitivity

Gravitational wave sensitivity



MAGIS-style satellite detector



Satellite detector concept

- Two spacecraft, MEO orbit
- Atom source in each
- Heterodyne laser link
- Resonant/LMT sequences

Example design

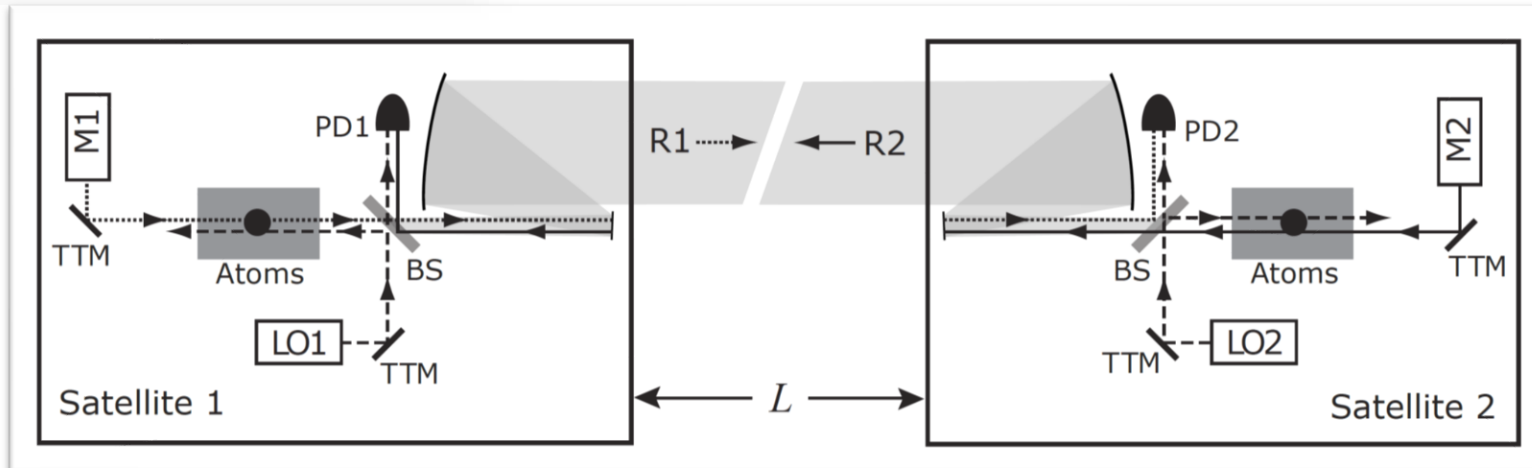
$$L = 4 \times 10^7 \text{ meters}$$

$$10^{-4} \text{ rad}/\sqrt{\text{Hz}}$$

$$\frac{n\hbar k}{m} T < 1 \text{ m}$$

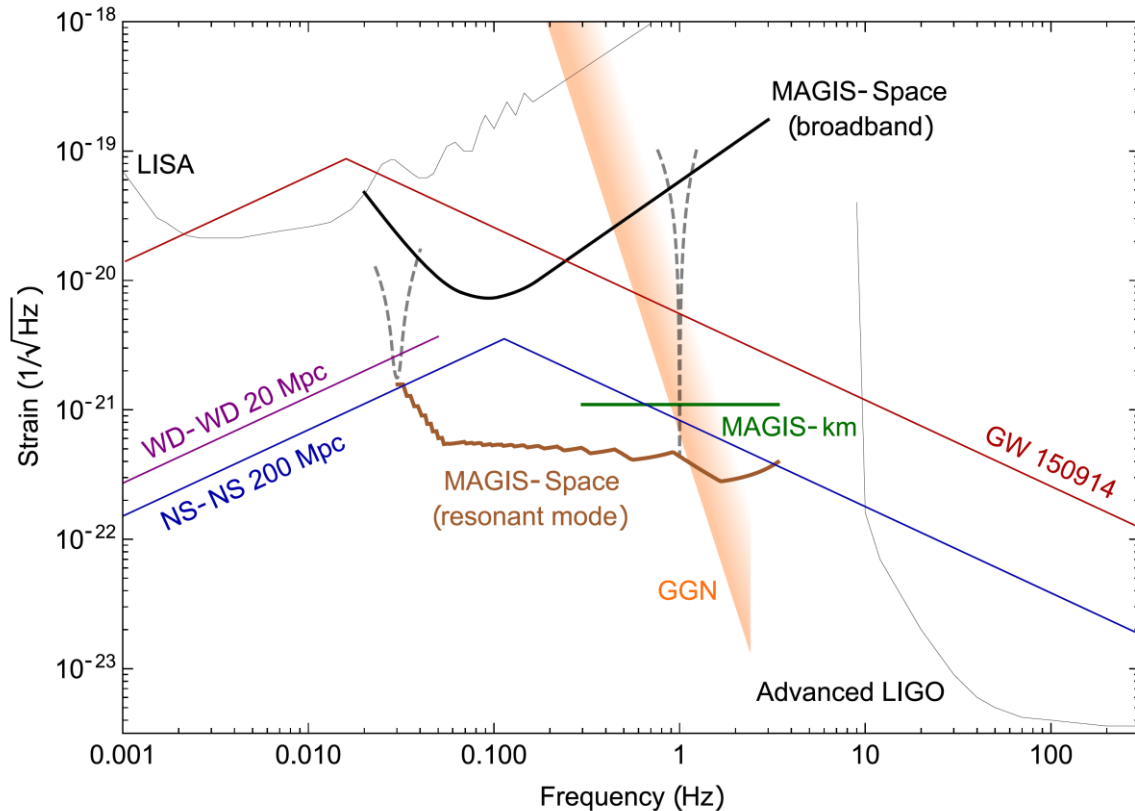
$$2TQ < 300 \text{ s}$$

$$n_p < 10^3$$



- Heterodyne link concept analogous to LISA (synthesize ranging between two test masses)
- Decouples atom-laser interaction strength from baseline length (diffraction limit)

Full scale MAGIS projected GW sensitivity



- Mid-band GW sources detectable from ground and space
- Gravity gradient noise (GGN) likely limits any terrestrial detector at low frequencies
- Longer baselines available in space reduce requirements (e.g., LMT), but can impact frequency response at high frequencies
- Flexible detection strategies possible (broadband vs resonant) with different tradeoffs in sensitivity/bandwidth

Development path

MAGIS detector development

Experiment	(Proposed) Site	Baseline L (m)	LMT Atom Optics n	Atom Sources	Phase Noise $\delta\phi$ (rad/ $\sqrt{\text{Hz}}$)
Sr prototype tower	Stanford	10	10^2	2	10^{-3}
MAGIS-100 (initial)	Fermilab (MINOS shaft)	100	10^2	3	10^{-3}
MAGIS-100 (final)	Fermilab (MINOS shaft)	100	4×10^4	3	10^{-5}
MAGIS-km	Homestake mine (SURF)	2000	4×10^4	40	10^{-5}
MAGIS-Space	Medium Earth orbit (MEO)	4×10^7	10^3	2	10^{-4}

**State of
the art**

Reaching required sensitivity requires extensive technology development in three key areas:

Sensor technology	State of the art	Target	GW sensitivity improvement
LMT atom optics	10^2	10^4	100
Spin squeezing	20 dB (Rb), 0 dB (Sr)	20 dB (Sr)	10
Atom flux	$\sim 10^6$ atoms/s	10^8 atoms/s	10

- Phase noise improvement strategy is a combination of increasing atom flux and using quantum entanglement (spin squeezing).
- LMT requirement is reduced in space proposals (longer baselines)